Dichroism and resonant diffraction in x-ray scattering by complex materials

2007 J. Phys.: Condens. Matter 19 213201

(http://iopscience.iop.org/0953-8984/19/21/213201)

IOP PUBLISHING JOURNAL OF PHYSICS: CONDENSED MATTER

J. Phys.: Condens. Matter **19** (2007) 213201 (22pp) doi:10.1088/0953-8984/19/21/213201

TOPICAL REVIEW

Dichroism and resonant diffraction in x-ray scattering by complex materials

S P Collins[1,2], **S W Lovesey**[3,4] **and E Balcar**[5]

[1] Diamond Light Source Ltd, Oxfordshire OX11 0QX, UK
[2] Department of Physics, Warwick University, Coventry CV4 7AL, UK
[3] ISIS Facility, RAL, Oxfordshire OX11 0QX, UK
[4] RIKEN Harima Institute, SPring-8, Hyogo 679-5148, Japan
[5] Vienna University of Technology, Atominstitut, Stadionallee 2, A-1020 Vienna, Austria

Received 2 November 2006, in final form 3 April 2007
Published 1 May 2007
Online at stacks.iop.org/JPhysCM/19/213201

Abstract

We survey universal concepts that influence dichroism and resonant Bragg diffraction, aiming to reach across the range of scientific disciplines that benefit from x-ray techniques, namely, chemistry, physics, life-sciences, and the science of materials. To this end, we adopt a top down discussion of the aspects of symmetry and concomitant selection rules. Starting from selection rules that can be deduced from the global condition that an observable quantity is unchanged on reversing the directions of both space and time separately, to selection rules that flow from bulk symmetry properties of electrons imposed by elements of a point group or crystal class to, finally, atomic selection rules that emerge from the details of the electronic structure. As a motivation for the latter we discuss, with a new calculation of the x-ray scattering length, $E1$–$M1$ absorption and scattering events that particularly interest scientists studying the chirality of life. In the main text there is modest use of mathematics, with appropriate details relegated to a few appendices.

Contents

1. Introduction

Techniques based on x-ray dichroism are well established, span the physical sciences and life-sciences, and routinely provide a wealth of scientific knowledge ranging from protein folding to nanomagnetism [1–7]. More recently, resonant x-ray Bragg diffraction has proved its worth [8, 9]. In particular, the two techniques, dichroism and resonant diffraction, have played a significant part in elucidating radical new properties of materials, including, high-T_c superconductivity, colossal magnetoresistance, and multiferroic modifications. The discovery of new electronic properties of materials has fuelled a resurgence of interest in atomic charge, spin and orbital degrees of freedom in systems of highly correlated electrons [6, 9, 10]. X-ray techniques offer a full view of these electron degrees of freedom and no other technique in the science of materials offers quite the same scope and accuracy.

Nature is daunting in the scale of complexity possessed by materials that surround us. Yet it is economical with general criteria of universal applicability, and we shall examine those that bear on dichroism and resonant diffraction in x-ray scattering. By and large, these general conditions stem from symmetry transformations and they create selection rules, which proscribe observations, e.g., the translation symmetry of a perfect crystal is the cause for Bragg's Law for diffraction intensities. Although outside of our main focus of interest here, it seems worth noting that, these same selection rules apply to and proscribe meaningful numerical simulations of an observable quantity, including a dichroic signal and a diffraction intensity.

Starting with Neumann's principle and global selection rules [5, 6, 11–13], we proceed to those derived from the macroscopic symmetry of a sample, and finally, we step down to examine the fine details and selection rules embedded in atomic calculations of observable quantities.

Absorption and diffraction are two sides of one coin, of course, since they have in common the x-ray scattering length, f [2, 14]. Absorption and its dependence on photon polarization and sample properties (dichroism), are related to the value of f in the forward direction, i.e., no deflection of the x-ray beam, and the intensity of a Bragg reflection is proportional to $|f|^2$.

To the casual interested reader, however, universal rules in studies of dichroism and diffraction are often obscured, partly by differences in the nature and size of the electronic systems under investigation, and by the relative importance of various resonance events, including electric dipole ($E1$), electric quadrupole ($E2$) and magnetic dipole ($M1$) [9, 15–17]. Perhaps even more confusing is the inconsistent language adopted to describe dichroic effects in different scientific disciplines.

The order of magnitude of the strength of an $E1$ resonance event is given by an atomic electric dipole ea_0, where a_0 is the Bohr radius, and the strength of an $M1$ event is given by a Bohr magneton $\mu_B = \alpha^2 a_0$, where α is the fine-structure constant $\approx 1/137$. Thus, the relative strengths of $E1$ and $M1$ are expressed by ratio $M1/E1 \approx \alpha/2$. The strength of an $E2$ event depends on the magnitude of the x-ray wavevector $q \approx 0.51E$ (keV) Å^{-1}, where E is the x-ray energy, and we achieve an estimate $E2/M1 \approx E/(27\text{ eV})$. These order of magnitude estimations take no account of radial integrals. In the case of an $M1$-event most integrals vanish. Our estimates are actually upper bounds that might be realized when electric events are more or less forbidden in the observed process [17].

Magnetic degrees of freedom possessed by electrons in a material can be polarized, by application of a magnetic field or through a spontaneous ordering of magnetic moments that is heralded by a phase transition. The fundamental signature of the magnetically polarized state is that the symmetry of time-reversal is broken, and this symmetry breaking manifests itself in a raft of observable effects, including the Faraday effect [18].

Some materials exist in structural units called enantiomers which are non-superimposable mirror images of each other, i.e., they are related like our left and right hands [13, 19–21]. The two units cannot be brought to coincide using ordinary rotation operations, of course, for they are interconverted by a change, or reversal, of parity. One enantiomer is called left and the other right and each enantiomer is said to possess a definite chirality ($\chi\epsilon\iota\rho$ = hand). An operational definition of a chiral unit is a unit whose image in a plane mirror cannot be made to coincide with itself [22]. The fundamental signature of such a modification is the lack of any mirror symmetry and the concomitant breaking of inversion symmetry. So-called chiral symmetry is seen to be the *actual absence* of a symmetry, namely, a lack of symmetry under improper rotations (rotation–inversions) [13], and a chiral material does indeed have lower symmetry than an achiral material. A chiral unit, or molecule, is said to be dissymmetric because of the absence of an axis of improper rotation, or all its symmetry properties are proper rotations. Such a unit is not necessarily asymmetric and devoid of symmetry, of course.

Left-handed and right-handed materials have identical properties, except when interacting with other chiral materials or chiral probes. Enantiomers of quartz ($P3_12$ (structurally right-handed) and $P3_22$ (structurally left-handed)) have opposite chirality (or handedness) and they rotate the polarization plane of light passing along the optical axis in opposite directions [12]. Sodium ammonium tartrate, famously studied by Pasteur [23], is one of few materials to self-resolve in a crystalline modification and it forms homochiral units when taken below 296 K. Natural circular dichroism arises from a partnership of specific signatures of the parity-odd properties of electrons and circular polarization (helicity) in the illuminating x-rays. Let us note that, a magnetic field has no chirality, and a magnetic field alone cannot resolve a racemic mixture into its enantiomers.

Analyses of observations from optical activity and natural circular dichroism have features in common, and a brief outline of optical activity merits its place in this article [5, 12, 19]. Optical activity and natural circular dichroism both arise from parity-odd processes in absorption, e.g., $E1$–$E2$ and $E1$–$M1$ processes. In a circularly polarized beam of light used for the observation of natural circular dichroism, the electric field direction rotates along the beam and it is a chiral phenomenon quantified by the helicity carried with the beam. Like helicity rotatory power is a pseudoscalar (a parity-odd scalar), which is derived from the observation of optical activity. However, this bulk observable is not an unambiguous signature of chirality since four crystal classes ($m, mm2, \bar{4}$, and $\bar{4}2m$) of the 15 crystal classes that allow optical activity are not enantiomorphous [12]. A signature of chirality of a molecule or a crystal that is unambiguous embraces additional information found in the space group.

A chiral unit possesses the symmetry of a self-enantiomeric space group, or a partner in one of the 11 enantiomorphic space group pairs, and all such space groups belong to one of the 11 enantiomorphous crystal classes. Many organic molecules are chiral, with the simplest amino acid in our body, glycine, a notable exception. Chiral molecules form enantiomorphous crystals of the corresponding handedness. Enantiomorphous crystals can also be built from achiral ion groups or molecules, e.g., quartz, $NaClO_3$ [24], $NaBrO_3$ [24], and tellurium [25]. The chlorate and bromate crystals possess the symmetry of the self-enantiomeric space group $P2_13$ and the two compounds, with identical chirality, rotate plane polarized light in opposite senses [24, 26].

The absolute structural configuration corresponding to a particular sense of optical rotation in enantiomorphic crystals can be determined by x-ray diffraction, if the crystal contains an ion which absorbs x-rays to an appreciable extent and anomalous scattering is observed [8]. Alternatively, neutron diffraction can be used to determine the absolute configuration [25]. The amplitude for scattering neutrons by the electrostatic field in a crystal includes a term that depends on the polarization of the beam, which arises from the spin–orbit interaction [27, 28].

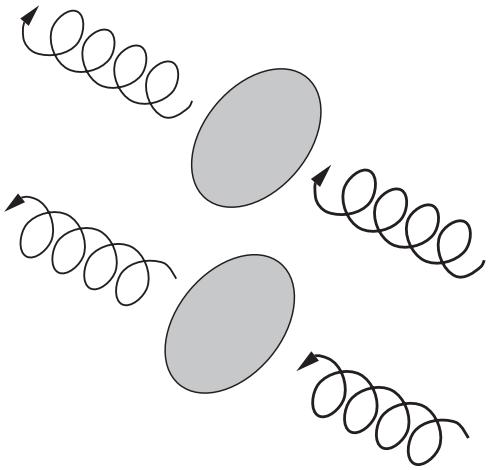

Figure 1. A conceptual circular dichroism experiment. The dichroic signal is the difference in absorption for the two opposite states of helicity.

In the cross-section, asphericity in the charge distribution in the spin–orbit term can cause interference with the amplitude for ordinary nuclear scattering to create a polarization dependence of the diffracted intensity. The polarization effect can be easier to measure than is the intensity difference between Bijvoet pairs [8], and it has been used to determine the absolute structural configuration that corresponds to a particular sense of optical rotation in a single crystal of tellurium [25] (enantiomorphic forms $P3_121$ and $P3_221$ which have opposite rotatory powers).

As a rule, living systems are constructed of only one of the two enantiomorhisms of biological molecules [1, 20, 21]. The exclusive use in terrestrial life of left-handed amino acids by proteins and right-handed sugars in DNA and RNA, and in metabolic pathways, is a pattern which is often called the homochirality of life [29, 30].

The origin of homochirality is one facet to the debate about the origin of living from nonliving matter, as by biopoiesis. An attempt to solve the issue of homochirality appeals to magnetochiral dichroism [5, 31] that arises in absorption by a material in which there is combined breaking of time-reversal and inversion. A notable feature of magnetochiral dichroism is its independence of the state of polarization of the x-rays.

In this paper we strive to find common ground between disparate features of the x-ray techniques. We first consider aspects of global symmetry, and draw what conclusions we can without making additional assumptions. Our next step is to consider the character of atomic spherical tensors that describe the various interaction processes, again underpinned by arguments of symmetry, and draw further conclusions regarding the general nature of these phenomena. For the most part, we can draw on established results and the main exception is our new and novel treatment of the scattering length for the $E1$–$M1$ process.

2. An orientation to dichroic signals

In the first few sections we discuss various global selection rules that affect the absorption coefficient and dichroic signals. Conceptually, an absorption experiment to observe circular dichroism is that illustrated in figure 1, where the dichroic signal is the difference in the absorption of two beams with opposite helicities.

Table 1. Transformations that preserve the line of propagation of the photon.

Transformation	Description	Picture	$(\mathbf{q}'/\mathbf{q},\ P_2'/P_2)$
1	None		$(+,+)$
$M_{\parallel}$	Mirror plane $\parallel$ to beam		$(+,-)$
$M_{\perp}$	Mirror plane $\perp$ to beam		$(-,-)$
$2_{\parallel}$	Twofold rotation about beam		$(+,+)$
$2_{\perp}$	Twofold rotation $\perp$ to beam		$(-,+)$
$\overline{1}$	Inversion	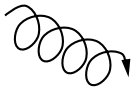	$(-,-)$
$\underline{1}\ (t \rightarrow -t)$	Time-reversal		$(-,+)$

One class of global rules is derived from a fundamental postulate that is often referred to as Neumann's principle [32]. It may be stated as follows: *an observable signal is forbidden if a symmetry operation applied to the physical system of interest modifies one aspect of the system and leaves all other aspects unchanged.* The physical system in question is the entire system, made up of the sample plus the radiation used in the observation, whose coordinates are those of both space and time. Observable properties of the entire system must be independent of coordinates and any symmetry transformation. An alternative perspective is that, f is a true scalar quantity and, as such, it must be invariant with respect to coordinate and symmetry transformations applied simultaneously to the electrons and the photons.

For the present discussion of global properties, the relevant coordinate transformations are the inversion of all spatial coordinates, an operation denoted by I, and the reversal of the direction of time, an operation denoted by θ [6, 9, 33]. (Looking ahead, in tables 1–3, inversion and time reversal are labelled according to the convention adopted in crystallography where they are denoted by an overbar and an underbar, respectively.) An observable quantity, e.g., a dichroic signal, cannot change when coordinates are merely renamed. Hence it follows that an observable is invariant with respect to I and θ applied separately. This conclusion is independent of the nature of forces that determine the properties of electrons, including parity-violating forces from weak neutral currents, for example [5, 34, 35]. Observables of interest here depend on both x-ray variables and electron variables and, obviously, we shall need to know how these variables react to I and θ. Indeed, we will find that the symmetry of an observable is a compound symmetry derived from the symmetry properties of all constituents.

States of polarization in a beam of photons are described by three, purely real Stokes parameters, P_1, P_2 and P_3 with $P_1^2 + P_2^2 + P_3^2 \leqslant 1$ and the equality is achieved by a fully polarized beam [2, 16]. P_3 defines linear polarization along two orthogonal directions in the plane normal to the beam, ξ ($P_3 = +1$, σ polarization) and η ($P_3 = -1$, π polarization). P_1

Table 2. The properties of four classes of electron variable under inversion or time-reversal.

	Inversion ($\mathbf{r} \to -\mathbf{r}$), denoted by I or $\overline{1}$	Time-reversal ($t \to -t$), denoted by θ or $\underline{1}$	Tensor rank K
1 (or $\mathbf{M}^2$ etc)	+	+	even K
U	−	+	all K
M	+	−	odd K
G	−	−	all K

Table 3. Symmetry transformations applied to dichroic signals with time-even electron variables. Plus (minus) signs indicate that the relevant electron or x-ray variable is unchanged (changed) by the symmetry transformation listed in the left-hand column, with no entry for the electron variable indicating no symmetry. Ticks and crosses indicate whether or not the signal is allowed for the given symmetry. The only symmetry signatures of the electron variables (**1**, **U**, etc) listed are those that are completely general and found in table 2. Signatures of the x-ray variable are not listed.

Symmetry, $\hat{S}$ (in addition to time-reversal)	P_2	**U**	**1**	Isotropic absorption	$P_2\mathbf{U}$ (natural circular dichroism)
1 (none)	+	+	+	✔	✔
$M_\parallel$	−		+	✔	✘
$M_\perp$	−		+	✔	✘
$2_\parallel$	+		+	✔	✔
$2_\perp$	+		+	✔	✔
$\overline{1}$	−	−	+	✔	✘

describes the linear polarization along directions at angles $\pm\pi/4$ to the ξ-axis. Finally, P_2 is the mean helicity in the photon beam. All Stokes parameters have the property that they do not change under the action of θ, i.e., P_1, P_2 and P_3 are time-even variables. With regard to inversion, or parity, P_1 and P_3 are true scalars and do not change under the action of I (parity-even) while P_2 is a pseudoscalar that changes sign under the action of I (parity-odd). The photon wavevector, **q**, is a polar vector (parity-odd) and time-odd. Additional properties of θ and a definition of the helicity operator, Σ, can be found in appendix A.

Properties of electrons in the sample can be usefully divided into those which are parity-even and those that are parity-odd, which may only occur in materials that possess a non-centrosymmetric structure. Bulk properties related to parity-odd processes, like optical activity, are forbidden in materials belonging to a centrosymmetric crystal class but this rule does not apply to the crystal structure factor for diffraction, except its value for forward scattering which is proportional to an absorption signal. Parity-even properties are observed in x-ray processes diagonal with respect to the resonance event determined by products of matrix elements of definite parity, such as $E1$–$E1$ and $E2$–$E2$. The magnetization, **M**, is parity-even (an axial vector) and it is time-odd. A time-even and parity-even property of the electrons is equivalent to an even power of **M**, while a time-odd and parity-even property is equivalent to an odd power of **M** and such a property is often simply referred to as a magnetic property of the electrons. We find that, for parity-even properties of the electrons there is a one-to-one correspondence between the rank and the exponent of the equivalent variable and its behaviour with respect to time-reversal; even rank is time-even and odd rank is time-odd (see, also, appendix A).

An interaction between x-rays and electrons which produces a dichroic signal can be a function of **q** and a Stokes parameter. Products of x-ray variables and variables

for electron properties that are invariant under the separate action of I and θ will lead to an allowed observable. Products with this property to be used in the following are the parity-even electron properties $P_3\mathbf{M}^{2n}$, linear dichroism, $\mathbf{q}P_2\mathbf{M}^{2n+1}$, magnetic circular dichroism (with n integer), and the parity-odd electron properties $P_2\mathbf{U}$, natural circular dichroism [4, 9, 15, 36–40], $\mathbf{qG}$, magnetochiral dichroism [9, 31, 39, 41, 42], and $\mathbf{q}P_3\mathbf{G}$, non-reciprocal dichroism [9, 39, 43, 44].

The distinction between reciprocal and non-reciprocal dichroism is behaviour with respect to the direction of propagation of the illuminating beam of x-rays. A reciprocal, or natural, dichroism is independent of the beam's direction whereas non-reciprocal dichroism changes sign when the beam's direction is reversed.

In the case of parity-odd electron properties, observed in processes that engage $E1$–$E2$ or $E1$–$M1$ events (products of parity-odd and parity-even matrix elements), the parity-even magnetization is no longer an appropriate equivalent variable. Instead, we use two parity-odd variables denoted by **U** ('ungerade') and **G** ('gerade') that are time-even and time-odd, respectively [9]. With respect to the combined action of I and θ, **U** and **M** behave alike, namely, they both change sign, and **U** is often called a polar variable. The symmetry properties of **G** match those of the magnetoelectric effect [9, 39, 41, 42]. Products of **q**, a Stokes parameter and **U** or **G** that are invariant under the separate action of I and θ have been given above.

Note that circular dichroic signals, proportional to P_2, observe either a magnetic property (parity-even) or a polar property (parity-odd) of the electrons. A measure of the actual chirality of the electrons is the scalar part of **U** and this variable is a pseudoscalar, of course. An applied magnetic field couples to time-odd variables, which are the magnetic and magnetoelectric variables. A field can be exploited to polarize a paramagnetic electron state, or reverse the polarity of a net spontaneous long-range magnetic order.

In the following sections we focus on selection rules that govern electron properties in the various forms of *circular* dichroism mentioned in the foregoing discussion. For example, we will demonstrate that, with natural circular dichroism there is a component of **U** which can be different from zero in a fluid sample. Later on, we recover the component of **U** in question from the description of the $E1$–$M1$ process in section 5.

3. Circular dichroism

We define circular dichroism as being the dependence of some x-ray interaction on the handedness of circular polarization, P_2, of the photon beam. Dichroic effects in x-ray attenuation by a material are illustrated in figure 1. While much of the underlying physics can be extended to other processes—one can speak of circular dichroism in x-ray scattering, photoemission etc—these phenomena involve additional vectors and are generally described by different atomic tensors.

Looking at figure 1, a circularly polarized monochromatic photon beam enters a sample, whose macroscopic shape is unimportant except for the thickness. The beam exits the sample in the same direction and with the same polarization, and it is monitored by a photon detector. In our idealized picture, where we neglect effects of linear dichroism, for example, the exit beam is considered to be identical to the incident beam to within a scale factor (we do not need to concern ourselves with the phase at this stage). The photon state is therefore in a pure state of the x-ray system.

The ratio of transmitted to incident intensity, or transmittance, is then

$$\frac{I}{I_0} = \mathrm{e}^{-\mu t}$$

where μ is the linear absorption coefficient and t is the sample thickness normal to the beam. The total cross-section, $\sigma_{\rm tot}$, and μ satisfy $\mu = N\sigma_{\rm tot}$, where N is the number density. This relation links a bulk property, μ, to a quantity that can be calculated for an atomic model of a material. $\sigma_{\rm tot}$ may be derived from the scattering length for the elastic scattering of x-rays by ions in the forward direction, with no change in polarization, which we denote by f_0. The actual relation, known as the optical theorem [14, 16], is an exact relation and it is $\sigma_{\rm tot} = 2\lambda\ {\rm Im}(f_0)$ where λ is the x-ray wavelength. Approximations of one kind or another in the calculation of f_0 are inevitable, of course.

We write the absorption coefficient as the sum of a term that is invariant with respect to helicity, P_2, and a term that reverses:

$$\mu = \mu_0 \pm \Delta\mu.$$

The object of the experiment is then to establish μ and $\Delta\mu$, both of which generally depend on the photon energy and sample orientation. The sample is said to exhibit circular dichroism if the dichroic signal $= \Delta\mu \neq 0$.

4. Selection rules for circular dichroism derived from sample symmetry

Let us consider under what circumstances knowledge of the symmetry of electrons in a sample is sufficient to state, with absolute confidence, that circular dichroism is *absent* in absorption. The only basic assumption to be made is that, all observable properties of electrons in the sample are invariant with respect to I and θ ($\overline{1} \Leftrightarrow I$, and $\underline{1}(t \rightarrow -t) \Leftrightarrow \theta$), even when the energy of the electrons includes a contribution from parity-violating forces that couple electrons and nucleons.

In order to enumerate the signals that are allowed for specified sample symmetries we appeal to Neumann's principle, once more. An observed signal is unchanged by a symmetry transformation, which we denote by $\hat{S}$. Recall, from section 2, that a dichroic signal is actually the product of x-ray variable(s) and an electron variable, e.g., magnetic circular dichroism is represented by $(\mathbf{q}P_2)(\mathbf{M})$. The action of $\hat{S}$ on a variable X is specified by a signature $s_{\rm x}$ that has values ± 1, and X is said to be unchanged by $\hat{S}$ when $s_{\rm x} = +1$. Using X for the x-ray variable(s) and E for the electron variable, with a signature $s_{\rm e}$, the principle is equivalent to the identity $s_{\rm x}s_{\rm e} = 1$. The sample symmetry is specified by $s_{\rm e} = +1$, i.e. the symmetry of electrons in the sample is *unchanged* by $\hat{S}$. With this premise, we simply enumerate signals that satisfy $s_{\rm x}s_{\rm e} = 1$. These signals, with $s_{\rm x} = +1$ and $s_{\rm e} = +1$, are allowed with the symmetry transformation $\hat{S}$.

We start by constructing symmetry transformations for a circularly polarized beam of x-rays, and any one of the transformations can be used for $\hat{S}$. By restricting the discussion to those transformations that preserve the line of propagation of a photon, one can define two useful scalar variables characteristic of a transformation: the ratio of the helicity (P_2'/P_2) of the transformed to original photon, and the corresponding ratio of wavevectors $(\mathbf{q}'/\mathbf{q})$. Each ratio has values ± 1, which we denote by $+$ or $-$. Table 1 lists the results of applying various transformations to a circularly polarized photon. The validity of the entries is possibly apparent by inspection of the pictorial representations of a circularly polarized photon. Alternatively, they may be derived from the symbolic relations, $I\Sigma = -\Sigma, \theta\Sigma = \Sigma, 2_\perp\Sigma = \Sigma, 2_\parallel\Sigma = \Sigma, I\mathbf{q} = -\mathbf{q}, \theta\mathbf{q} = -\mathbf{q}, 2_\perp\mathbf{q} = -\mathbf{q}$ and $2_\parallel\mathbf{q} = \mathbf{q}$, together with $M_\parallel = I\otimes 2_\perp$ and $M_\perp = I\otimes 2_\parallel$. Note that time-reversal, θ, and a twofold rotation perpendicular to the propagation vector, $2_\perp$, are equivalent symmetry transformations of a photon. Recall that, P_2 is the value of the helicity operator, Σ, averaged over states of polarization (see, also, appendix A).

Although table 1 shows some symmetry properties of just one specific photon polarization state (right-handed circular), it provides the building blocks for describing the symmetry of any

Table 4. Symmetry transformations applied to dichroic signals with time-odd electron variables. The right-hand column lists the constraint placed on **M** by the specified sample (electron) symmetry.

Symmetry, $\hat{S}$	P_2	**q**	**M**	**G**	$\mathbf{q}P_2\mathbf{M}$ (magnetic circular dichroism)	**qG** (magneto-chiral dichroism)	Comment on vanishing magnetic circular dichroism
1	+	+	+	+	✔	✔	
$M_\parallel$	−	+			✘	✔	$\mathbf{M} \perp \mathbf{q}$
$\underline{M}_\parallel$	−	−			✔	✘	
$M_\perp$	−	−			✔	✘	
$\underline{M}_\perp$	−	+			✘	✔	$\mathbf{M} \perp \mathbf{q}$
$2_\parallel$	+	+			✔	✔	
$\underline{2}_\parallel$	+	−			✘	✘	$\mathbf{M} \perp \mathbf{q}$
$2_\perp$	+	−			✘	✘	$\mathbf{M} \perp \mathbf{q}$
$\underline{2}_\perp$	+	+			✔	✔	
$\overline{1}$	−	−	+	−	✔	✘	
$\underline{\overline{1}}$	−	+	−	+	✘	✔	$\mathbf{M} = 0$

pure state of polarization, which can be written as a coherent sum of the right- and left-handed amplitudes (helicity eigenstates). In this paper, we do not discuss, explicitly, dichroic effects that couple to linear polarization. We will consider effects which couple to an unpolarized beam (i.e. magnetochiral dichroism). Such a beam can be realized by taking an incoherent sum of right- and left-handed states.

Symmetry properties of the electrons are contained in the relevant crystal class or point group, and they are far more varied than those of an x-ray beam, discussed above. Electron degrees of freedom in a sample are represented by equivalent variables that are usually expectation values of spherical tensor operators. Our choice of variables is discussed in section 2 and they are gathered in table 2. For the present development, all we need to note are their signatures with respect to inversion and time-reversal. In table 2, parity-even (parity-odd) is labelled $+(-)$, and the same labelling scheme is used for time-even and time-odd. In general, the sample will contain variables that have no definite symmetry with respect to these operations and will then be described by a sum of these basic variables.

We can now enumerate signals that are allowed by specified sample symmetry. The basic symmetry transformations are listed in table 1. Tables 3 and 4 list the symmetry of various x-ray and electron variables, and whether or not the resulting signals are allowed, based on the premise that the electron variable is unchanged.

The construction of entries in the tables merits comment. A $-$ sign is used in the tables to label an electron variable that is changed by specific sample symmetry, $\hat{S}$. By definition, the corresponding signal is forbidden and marked ✘, e.g., in table 3, $P_2\mathbf{U}$ is forbidden for sample symmetry $\overline{1}$ because **U** is parity-odd with $-$ in the column labelled **U**. An electron variable unchanged by $\hat{S}$ is not observed should $\hat{S}$ change the corresponding x-ray variable(s), e.g., in table 4 magnetic circular dichroism (MCD) is a forbidden signal for sample symmetry $M_\parallel$ because the product of the corresponding x-ray variables is changed by $M_\parallel$.

While only four classes of signal are described, we should point out that these are archetypal examples that represent all signals with the same x-ray and sample symmetries under inversion and time-reversal. For example, signals that are independent of polarization share the same symmetry properties as those which scale with P_1 or P_3; terms which are of even power in **M** are even with respect to both I and θ and can be represented by the symbol, **1** (sometimes

Table 5. Symmetry transformations for a fluid applied to time-even electron variables, and the corresponding dichroic signals. Shown in brackets in the left-hand column are specific cases of a more general transformation, which cause some signals to vanish.

Symmetry, $\hat{S}$ (in addition to time-reversal)	**1** (isotropic)	$P_2\mathbf{U}$ (natural circular dichroism)
1	✔	✔
$\mathbf{M}(M_\parallel, M_\perp)$	✔	✘
2	✔	✔
$\overline{1}$	✔	✘

omitted). For example, the item **1** in table 2 can represent either isotropic absorption or linear dichroism, $P_3\mathbf{M}^2$, although the condition for the resulting signal to vanish may differ due to the different transformation properties of the x-ray variable under reflection or rotation.

Next, let us consider dichroic signals for a spatially isotropic and homogeneous sample; fluids of randomly oriented, identical molecules or fine grains constitute such a sample. We remain focused on the symmetry properties of the constituent parts of the fluid. Specific directions in the symmetry transformations of a fluid are meaningless, of course. If a constituent possesses a mirror plane the fluid is totally symmetric with respect to any mirror plane, for example. Should any mirror plane of symmetry cause a signal to vanish, the signal from the fluid vanishes. It is therefore a relatively simple matter to extend the above tables to fluids. Signals that are created by a fluid with time-even electron variables are given in table 5.

A fluid with time-odd electron variables is more interesting. Consider first a fluid not perturbed by the coupling of time-odd electron variables to an external field. Such a sample is unchanged by any spatial rotation, of course. But the relevant x-ray variables ($\mathbf{q}$ and $\mathbf{q}P_2$) are changed by a rotation, namely, $2_\perp$. Thus, an unperturbed fluid with time-odd electron variables does not create dichroic signals.

We next turn to a fluid, with time-odd electron variables, that is polarized by an external magnetic field. Let the field be perpendicular to $\mathbf{q}$, say. The spatial symmetry of the fluid is reduced by the polarization induced in the electron variables. However, the fluid remains unchanged by a rotation that causes the relevant x-ray variables to change, a rotation $2_\perp$ which is a symmetry transformation of both the intrinsic fluid and the external field. So, a (magnetic) fluid with time-odd electron variables that has field-induced polarization perpendicular to $\mathbf{q}$ does not create dichroic signals.

The situation is quite different if the applied field is parallel to $\mathbf{q}$. There is no obvious argument in this case to suggest that dichroic signals vanish, and in general, they do not. To enumerate the allowed signals, we consider a fluid whose randomly oriented constituent parts possesses symmetry transformations that are consistent with the symmetry of the applied field, i.e. invariance with respect to any rotation about $\mathbf{q}$. The allowed signals are summarized in table 6. In this table, we indicate the general symmetry of the electron variable and, in brackets, the specific sample symmetry that is consistent with the external field. It is the latter that determine whether or not the dichroic signals of interest are forbidden.

Tables 3–6 reveal a surprisingly large number of important results, considering that we have yet to discuss specific underlying physical mechanisms. Some noteworthy conclusions are summarized below.

Oriented samples and time-even electron variables:

- Natural circular dichroism (NCD) is ruled out by inversion symmetry.
- Although NCD is ruled out in the presence of mirror symmetry perpendicular or parallel

Table 6. Symmetry transformations for a fluid applied to time-odd electron variables and corresponding dichroic signals, with an external magnetic field parallel to **q**.

Symmetry $\hat{S}$	$\mathbf{q}P_2\mathbf{M}$ (magnetic circular dichroism)	**qG** (magnetochiral dichroism)
1	✔	✔
$\mathbf{M}(M_\perp)$	✔	✘
$\underline{\mathbf{M}}(\underline{M}_\parallel)$	✔	✘
2	✔	✔
$\underline{2}$	✔	✔
$\overline{1}$	✔	✘

to the beam, it is not ruled out for a general mirror plane. NCD in oriented samples cannot, therefore, be identified as a uniquely chiral phenomenon of the sample.

- NCD is invariant with respect to twofold rotations about the beam, or perpendicular to it.

The latter point is not immediately apparent from table 3. However, we note that P_2 is invariant with respect to $2_\perp$. Moreover, the observable dichroic quantity, $P_2\mathbf{U}$, must be invariant with respect to all symmetry operations. This requires that **U** in $P_2\mathbf{U}$ must be invariant with respect to $2_\perp$.

Oriented samples and time-odd electron variables (magnetic crystals):

- Magnetic circular dichroism (MCD) is forbidden when **M** (which we can identify with the sample magnetic vector) vanishes, or lies perpendicular to the beam.
- MCD reverses under twofold rotation of the sample perpendicular to the beam ($2_\perp$).
- Magnetochiral dichroism (MχD), which couples an unpolarized (or linearly polarized) beam to the time- and parity-odd magnetoelectric variable, **G**, vanishes if the sample possesses either parity or time-reversal as separate symmetries. However, MχD is allowed if these two symmetry transformations appear in the combination $I\theta$.
- MχD is generally allowed with oriented samples that possess mirror symmetry. In consequence, MχD is not identified as a true chiral signal in this instance.

Fluid samples:

- NCD for fluids vanishes for all non-chiral sample symmetries ($M_\perp$, $M_\parallel$ and $\overline{1}$), and the signal is therefore identified as a true chiral effect.
- No dichroic signals arise from a fluid, with time-odd electron variables, which is unpolarized (zero applied magnetic field).
- No dichroic signals arise from a fluid, with time-odd electron variables, which is polarized by a magnetic field applied in a direction that is perpendicular to the x-ray beam.
- MχD from a fluid with time-odd electron variables, subjected to an applied magnetic field, is forbidden for all non-chiral symmetries ($M_\perp$, $\underline{M}_\parallel$ and $\overline{1}$). MχD is therefore identified as a true chiral signal, in this particular instance.

5. Atomic calculations

To step beyond the macroscopic descriptions of dichroism and scattering in previous sections, one can appeal to atomic models. Such models have a long and distinguished record of success in the analysis of observations on the electronic properties of materials made by techniques that include ESR, NMR, Mössbauer spectroscopy, muon spectroscopy, and the scattering of neutrons and x-rays [9, 27, 33, 45].

To each ion in the model of the material one associates an atomic tensor [33, 45]. For a crystalline material, the central object is a unit cell, and the unit cell structure factor, F, contains a sum over all ions in the cell and their associated tensors. A manifestation of Neumann's principle is that, F possesses the symmetry of the point group of the crystal of which there are 32 non-magnetic crystal classes. Within the context of an atomic model of a material, F describes all bulk properties. To analyse diffraction, a spatial phase factor accompanies each tensor and the structure factor is different from zero when the Bragg wavevector, defined by Miller indices h, k, l, coincides with a reciprocal lattice vector indexed by one of the 230 space groups. In general, atomic tensors in the unit cell are not related simply by translations because sites in the cell may have different local environments. A change in translation symmetry leads to additional Bragg reflections, e.g., purely magnetic superlattice reflections in diffraction by an antiferromagnet or weak Bragg reflections that arise from angular anisotropy in the electron valence states [46–48].

A dichroic signal is proportional to $F(h, k, l)$ with $h = k = l = 0$, and formally this dimensionless quantity is an inverse energy moment of the x-ray absorption cross-section, or the imaginary part of the forward scattering length. The energy integration is carried out over a small interval of energy in the vicinity of the relevant absorption edge. $F(0, 0, 0)$ can be expressed in terms of expectation values, or time averages, of atomic variables and the expressions constitute the celebrated sum rules of Thole *et al* [6, 49, 50] that apply to dichroic signals from spin–orbit split intervals of the x-ray absorption spectrum. Intensity in a Bragg reflection is proportional to $|f|^2$, where f is the scattering length. Quite often, it is adequate to describe Bragg diffraction that is enhanced by a resonance event at an energy Δ by $f \approx -\Delta r_e F(h, k, l)/(E - \Delta + i\Gamma/2)$ where r_e is the classical radius of an electron, E is the x-ray energy and Γ is the total width of the resonance. The linear absorption coefficient is $\mu = (4\pi n_0/q)\mathrm{Im}(f)$, where n_0 is the density of resonant scatterers. Using this expression for μ and representing f by a single oscillator one finds $\int(\mu/E)\mathrm{d}E \approx (4\pi^2 n_0 r_e/q)F$.

Having briefly reviewed the central role of $F(h, k, l)$ in the analysis of dichroic signals and Bragg diffraction patterns let us elaborate on the form it takes in the context of an atomic model. Atomic tensors are labelled by their rank, K, which is a positive integer. The sum within the unit cell of tensors associated with ions that engage in a resonance event, at an energy Δ, is here called $\mathbf{\Psi}^K(h, k, l)$ and $F = \sum_K \mathbf{X}^K \cdot \mathbf{\Psi}^K(h, k, l)$ where $\mathbf{X}^K$ is a spherical tensor that depends on properties of the primary and secondary x-rays [51]; see (6.3). We use $\mathbf{X}^K$ to describe $E1$–$E1$ resonance events and $\mathbf{H}^K$ [52] to describe $E2$–$E2$ events, and expressions for these tensors are provided in [9] for the four channels of polarization. The $E1$–$E1$ and $E2$–$E2$ events are parity-even, for they are products of matrix elements with definite parity.

Parity-odd events, such as $E1$–$M1$ and $E1$–$E2$, are similarly described within the framework of an atomic model [9, 15, 39]. The only difference is a need to employ symmetric, $\mathbf{G}^K$, and antisymmetric, $\mathbf{U}^K$, atomic tensors that appear in $F(h, k, l)$ with their own x-ray factors. A calculation of $F(h, k, l)$ for the $E1$–$E2$ event is described in [9] and later in this paper we give results from a corresponding calculation for the $E1$–$M1$ event.

Core-hole events possess selection rules that stem from the angular momentum transferred in the photoelectron event [17]. $E1$ and $E2$ events involve one and two units, respectively. Absorption at the K-edge and an $E2$ event form a powerful probe of 3d transition metal ions because the observed signal is directly related to multipole moments of the 3d valence shell [53]. In addition, the resonant energy is equivalent to an x-ray wavelength that matches the separation of ions in a crystal and several Bragg reflections can be observed. At a K-edge, the spin–orbit interaction is zero and there is no splitting of the core state by this interaction. In consequence, an $E2$ dichroic signal or a Bragg diffraction pattern relate to properties of the orbital angular momentum in the 3d valence shell, to a good approximation.

The number of multipoles accessed in an observation is a direct consequence of the triangle rule applied to the x-ray operators. $E1$ and $E2$ operators are tensors of rank 1 and 2, respectively. $E1$–$E1$, $E1$–$E2$ and $E2$–$E2$ events sample multipoles with ranks $K = 0, 1$, and 2, $K = 1, 2$, and 3, and $K = 0, 1, 2, 3$ and 4, respectively. $E1$–$M1$ and $E1$–$E1$ events contain multipoles with the same ranks although the physical contents of the multipoles are very different since the former event is parity-odd and the latter is parity-even. Recall that, multipoles in a parity-even event have a time signature that is related to the rank, and even-rank (odd-rank) multipoles are time-even (time-odd). On the other hand, in a parity-odd event the multipoles $\mathbf{G}^K$ and $\mathbf{U}^K$ for all K are time-odd and time-even, respectively.

Expressions for dichroic signals are provided and discussed in several places [5, 6, 9, 39]. In consequence, here we do no more than record a few key results by way of specific illustrations of topics already discussed.

In our chosen coordinate system the z-axis is parallel to the x-ray beam, and $\hat{q}_0$ is the unit wavevector. Linear polarization $P_3 = +1$ is parallel to the x-axis. A dichroic signal is the change on reversing polarization in the linear absorption coefficient. In dimensionless form, the change ΔF through engaging an $E1$ event and averaging over states of polarization in the x-ray beam is,

$$(\Delta F(E1\text{–}E1))_{\rm av} = -\frac{1}{\sqrt{2}}\hat{q}_0 P_2 \Psi^1_0 + \frac{1}{2} P_3 \left(\Psi^2_{+2} + \Psi^2_{-2}\right). \tag{5.1}$$

The two contributions to the right-hand side are the circular and linear dichroic signals, respectively. $\Psi^K_Q(h, k, l)$ with $-K \leqslant Q \leqslant K$ is evaluated for zero deflection of the x-ray beam for which $h = k = l = 0$. The circular dichroic signal vanishes if there is no net magnetization in the direction of the beam. $\Psi^2_{\pm 2}$ account for the linear dichroic signal and describe quadrupole-like structure factors with components in the plane normal to the beam. In terms of equivalent Cartesian tensors one finds $\Psi^2_{+2} + \Psi^2_{-2} \propto \Psi^2_{xx} - \Psi^2_{yy}$. Evidently, the linear dichroic signal is zero for an isotropic or a metrically cubic material. Sum rules tell us that summed over the spin–orbit split core states, $\Psi^1_0 \equiv \Psi^1_z$ is proportional to the orbital magnetization in the z-direction. Contributions at the edges are distinguished by spin and spin anisotropy tensors of opposite sign [50, 54].

Turning to dichroism caused by a pure $E2$ event we give one important example. The circular dichroic signal at the K-edge of a 3d transition metal ion is directly related to dipole ($K = 1$) and octupole ($K = 3$) moments of the orbital magnetization in the 3d shell. One finds, for this particular case,

$$(\Delta F(E2\text{–}E2))_{\rm av} = \frac{1}{2\sqrt{10}}\hat{q}_0 P_2 \left(\Psi^1_0 - 2\Psi^3_0\right). \tag{5.2}$$

We conclude this section with a brief survey of dichroic signals created by an $E1$–$E2$ event that can arise for non-centrosymmetric crystals [9, 15, 39]. Structure factors for the parity-odd contributions are $\mathbf{\Psi}^{K,g}$ and $\mathbf{\Psi}^{K,u}$, as in (6.6) and (6.7), where superscripts denote symmetric (time-odd) and antisymmetric (time-even) atomic tensors, respectively.

Natural circular dichroism is proportional to $P_2\Psi^{2,u}_0(0, 0, 0)$. The structure factor $\Psi^{2,u}_0(0, 0, 0)$ is the sum of pseudotensors $\langle U^2_0\rangle$ which are often referred to as an axial toroidal quadrupole. An operator equivalent for $\mathbf{U}^2$ represents it as a product of orbital angular momentum, $\mathbf{L}$, and the orbital anapole, $\mathbf{\Omega} = \mathrm{i}[\mathbf{L}^2, \mathbf{n}]$, where $\mathbf{n}$ is a unit polar vector [10, 15, 39]. Note that, $\mathbf{L}$ and $\mathbf{\Omega}$ are orthogonal variables with $\mathbf{L}\cdot\mathbf{\Omega} = 0$. The sum $\Psi^{2,u}_0$ is zero if the crystal class includes mirror symmetry.

One such case is the corundum structure $R\bar{3}c$ that is appropriate to the archetypal magnetoelectric material Cr_2O_3 [11, 41, 42, 55, 56]. Although $\mathbf{\Psi}^{2,u}(0, 0, 0) = 0$ the sum can be different from zero for a class of Bragg reflections that include $h = k = 0$ and $l = 2n + 1$.

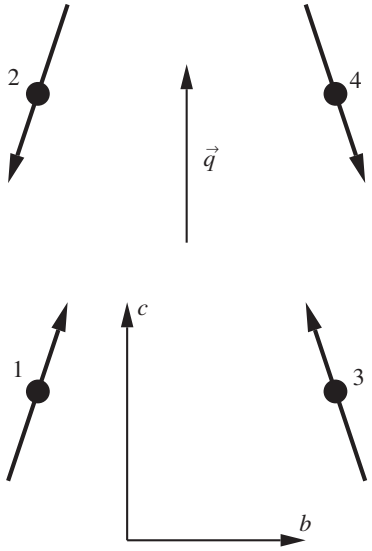

Figure 2. A projection onto the *b*–*c* plane of four sites in a cell and the magnetic dipole moments associated with the sites. Moments lie in the plane of the figure, that is taken to be the *b*–*c*-plane of the cell. An x-ray beam is directed along the *c*-axis.

The contribution to diffraction by Cr_2O_3 appears in channels with rotated polarizations, and it has opposite signs in the two such channels, $\pi'\sigma$ and $\sigma'\pi$ [9, 48, 57]. The sign difference can be assigned to opposite handedness in $\pi'\sigma$ and $\sigma'\pi$.

Non-reciprocal linear dichroism caused by an $E1$–$E2$ event is proportional to $\hat{q}_0 P_3\{\mathrm{i}(\Psi^{2,g}_{+2} - \Psi^{2,g}_{-2}) - \sqrt{2}(\Psi^{3,g}_{+2} + \Psi^{3,g}_{-2})\}$ and it can be different from zero for materials that support a long-range magnetic order. The combination $(\Psi^{2,g}_{+2} - \Psi^{2,g}_{-2})$ behaves like a quadrupole moment with x–y spatial symmetry. Both contributions to the dichroic signal vanish if the point group excludes diad axes. Note that $\langle \mathbf{G}^2 \rangle$ and $\langle \mathbf{G}^3 \rangle$ are, respectively, pseudotensors and true tensors, and their contributions to non-reciprocal dichroism differ in phase by 90°.

The magnetochiral dichroic signal is controlled by the quantity $\hat{q}_0\{\Psi^{1,g}_0 - (2/3)^{1/2}\Psi^{3,g}_0\}$, which is independent of polarization in the x-ray beam. Switching an applied magnetic field, thereby reversing the sign of magnetoelectric tensors, affords a method of distinguishing a magnetochiral, $E1$–$E2$ contribution to the absorption coefficient.

By way of an example we consider a non-centrosymmetric cell of four ions that is sketched in figure 2. The cell and the configuration of magnetic moments arise in a conceptual modification of a perovskite structure. By tuning the x-ray energy, contributions to dichroic signals and diffraction come from four ions at sites $\mathbf{d}_1 = (0, 0, 0)$, $\mathbf{d}_2 = (0, 0, 1/2)$, $\mathbf{d}_3 = (1/2, 1/2, 0)$, and $\mathbf{d}_4 = (1/2, 1/2, 1/2)$. In figure 2, the a-axis is normal to the plane of the diagram and the magnetic moments, represented by arrows, lie in the b–c-plane. The motif of moments is derived by taking site 1 as origin and generating the environment at site 2 by application of time-reversal, θ. The environment at site 3 is generated by a rotation by π about the c-axis, an operation denoted by C_{2z}. Sites 3 and 4 are related by θ, of course. There is no net magnetization, because magnetic moments can be grouped in pairs along the c-axis with opposite moments. As described, the model has a unique (polar) axis and a ferroelectric modification is allowed. One finds $\Psi^{K,u}_Q(0, 0, 0) = 4\langle U^K_Q \rangle$ with even Q, and $\Psi^{K,g}_Q(0, 0, 0) = 0$. In consequence, natural circular dichroism is allowed and dichroic signals from magnetoelectric tensors are forbidden.

The dichroic response of the cell is changed by the addition of inversion to the symmetry at sites 2 and 4, which makes the structure centrosymmetric. One finds $\Psi_Q^{K,u}(0,0,0) = 0$ and $\Psi_Q^{K,g}(0,0,0) = 4\langle G_Q^K\rangle$ with even Q. Several aspects of this modification merit comment. First, the introduction of inversion symmetry rules out the possibility of a ferroelectric state. Secondly, time-reversal and inversion are combined and a magnetoelectric state is allowed. Thirdly, in the model, time-reversal and C_{2x} are equivalent operations as the magnetic moments are confined to the b–c-plane. Since IC_{2x} is equivalent to a mirror plane natural circular dichroism is forbidden, which is confirmed by finding $\Psi_Q^{K,u}(0,0,0) = 0$. These results depend on the direction of the beam which in figure 2 is parallel to the c-axis. If the beam were rotated to lie along the b-axis, for example, the magnetochiral and non-reciprocal dichroic signals vanish.

6. $E1$–$M1$ scattering length

$M1$ transitions occur only at relatively low excitation energies [15, 17]. To a good approximation, $M1$ transitions can be neglected in core-level events, considered thus far, for they depend on the influence of the configuration interaction. A matrix element of the magnetic moment operator, $\boldsymbol{\mu}$, vanishes unless the orbital angular momentum is the same in its two states. Also, a matrix element of $\boldsymbol{\mu}$ is proportional to the radial overlap of the two states and there are no contributions to an $M1$ event from orthogonal orbitals [17]. Even so, analysis of the observation of circular dichroism by a randomly oriented system suggests that core transitions at the K-edge can enable $E1$–$M1$ events [58]. In the experiment, natural circular dichroism was claimed at the carbon K-edge (∼290 eV) of methyloxirane in the vapour phase.

An analysis of the $E1$–$M1$ contribution to the scattering length in the framework of an atomic model quickly reveals the salient features. However, the resulting expression for the scattering length is not a promising starting point for *ab initio* calculations unless the majority of contributing electron states are spatially localized.

The $E1$–$M1$ structure factor is derived from the dimensionless quantity [9],

$$Z(E1\text{–}M1) = \frac{1}{2}\sum_{\eta}\sum_{jj'}\left\langle\left\{\boldsymbol{\epsilon}'\cdot\mathbf{R}_j|\eta\rangle\langle\eta|(\mathbf{q}\times\boldsymbol{\epsilon})\cdot\boldsymbol{\mu}_{j'} + (\mathbf{q}'\times\boldsymbol{\epsilon}')\cdot\boldsymbol{\mu}_j|\eta\rangle\langle\eta|\boldsymbol{\epsilon}\cdot\mathbf{R}_{j'}\right\}\right\rangle. \tag{6.1}$$

Here, $\mathbf{R}_j$ and $\boldsymbol{\mu}_j = (\mathbf{L} + 2\mathbf{S})_j$ are the position and magnetic moment of the electron labelled by the index j. The primary x-rays have polarization $\boldsymbol{\epsilon}$ and wavevector $\mathbf{q}$, with $\mathbf{q}\cdot\boldsymbol{\epsilon} = 0$, and a prime is used to denote the quantities that characterize secondary x-rays. Intermediate states visited in an $E1$–$M1$ event are labelled η in (6.1), and outer angular brackets denote the mean value, or time-average value.

Two x-ray factors arise in (6.1), one of which is formed by the vectors $(\mathbf{q}\times\boldsymbol{\epsilon})$ and $\boldsymbol{\epsilon}'$ and the second factor is derived from the first by exchanging primed and unprimed variables. Let us define a spherical tensor,

$$\tilde{M}_Q^K = \left\{(\hat{\mathbf{q}}\times\boldsymbol{\epsilon})\otimes\boldsymbol{\epsilon}'\right\}_Q^K, \tag{6.2}$$

where $\otimes$ denotes a tensor product (appendix A) [59–61] and $\hat{\mathbf{q}} = \mathbf{q}/q$. It is convenient for us to express $\tilde{M}_Q^K$, and its counterpart M_Q^K, obtained by exchanging primed and unprimed x-ray variables, in terms of a tensor formed from the polarization vectors, namely,

$$X_Q^K = \left(\boldsymbol{\epsilon}'\otimes\boldsymbol{\epsilon}\right)_Q^K = (-1)^K\tilde{X}_Q^K. \tag{6.3}$$

The rank K in (6.2) and (6.3) has values $K = 0$, 1 and 2. One can show that,

$$\tilde{M}^K_Q \pm M^K_Q = -\mathrm{i}\sqrt{6}\sum_{K'Q'}(2K'+1)^{1/2}\begin{Bmatrix} K & K' & 1 \\ 1 & 1 & 1 \end{Bmatrix} \times X^{K'}_{Q'}\sum_{\nu}(\hat{q}_\nu \pm (-1)^{K'}\hat{q}'_\nu)(K'Q'1\nu|KQ). \tag{6.4}$$

The Clebsch–Gordan coefficient and $6j$-symbol are here defined in accord with Edmonds [59] and Judd [60]. The linear combinations of $\tilde{M}^K_Q$ and M^K_Q given in (6.4) are exactly what is needed in the structure factor, as we shall now demonstrate.

The quantity $Z(E1\text{–}M1)$ defined in (6.1) is evidently of the form,

$$Z(E1\text{–}M1) = \sum_K \left\{\tilde{\mathbf{M}}^K \cdot \langle \boldsymbol{\Upsilon}^K\rangle + \left(\mathbf{M}^K \cdot \langle \boldsymbol{\Upsilon}^K\rangle\right)^*\right\} \tag{6.5}$$

where $\boldsymbol{\Upsilon}^K$ is a spherical tensor operator that represents the properties of the electrons. The mean value $\langle \boldsymbol{\Upsilon}^K\rangle$ is a linear combination of matrix elements of $\mathbf{R}$ and $\boldsymbol{\mu}$ and appendix B contains an explicit expression. $\tilde{M}^K_Q$ satisfies $(\tilde{M}^K_Q)^* = (-1)^{K+Q}\tilde{M}^K_{-Q}$ and there is a similar result for M^K_Q.

The operators $\boldsymbol{\Upsilon}^K$ for electrons do not have conventional properties because (6.5) is not yet cast in a form that clearly displays the role of time-reversal combined with inversion. The conjugate operation for x-ray variables is known as the crossing transformation that includes an exchange of variables $\boldsymbol{\epsilon}$, $\boldsymbol{\epsilon}'$, $\hat{\mathbf{q}}$, $\hat{\mathbf{q}}'$, P_1, P_2, P_3 with $\boldsymbol{\epsilon}'$, $\boldsymbol{\epsilon}$, $\hat{\mathbf{q}}'$, $\hat{\mathbf{q}}$, P_1, $-P_2$, P_3 [16]. An individual contribution to $Z(E1\text{–}M1)$ must be unchanged by the simultaneous action, on the appropriate atomic tensor, of time-reversal and inversion, and the crossing transformation applied to $\tilde{\mathbf{M}}^K$ and $\mathbf{M}^K$. The effect of the crossing transformation is summarized by $\tilde{\mathbf{M}}^K \leftrightarrow \mathbf{M}^K$, and the linear combinations in (6.4) are symmetric (+) and antisymmetric (−) with respect to the transformation. The symmetric combination $\tilde{\mathbf{M}}^K + \mathbf{M}^K$ must be paired with our choice for the magnetoelectric tensors, $\mathbf{G}^K$, that are symmetric with respect to the combined action of I and θ, and $\tilde{\mathbf{M}}^K - \mathbf{M}^K$ must, similarly, be paired with polar tensors, $\mathbf{U}^K$, that are antisymmetric with respect to the combined action of I and θ. We have defined $\mathbf{G}^K$ and $\mathbf{U}^K$ to possess the property $\langle G^K_Q\rangle^* = \langle (G^K_Q)^+\rangle = (-1)^Q\langle G^K_{-Q}\rangle$ and $\langle U^K_Q\rangle^* = (-1)^Q\langle U^K_{-Q}\rangle$. This property enters our definition of time-even and time-odd, namely, an operator O is even or odd according to the sign in $\theta O\theta^{-1} = \pm O^+$.

The appropriate expression for $\langle \Upsilon^K_Q\rangle$ to use in (6.5) is derived by examination of the matrix element reported in appendix B. One finds $\langle \Upsilon^K_Q\rangle = \mathrm{i}^{K-1}[\langle U^K_Q\rangle - \mathrm{i}\langle G^K_Q\rangle]$ and here the phase factor depends on our choice for Hermitian conjugates of $\mathbf{U}^K$ and $\mathbf{G}^K$. Properties of the electrons that can participate in a parity-odd event are represented by structure factors,

$$\Psi^{K,g}_Q = \sum_{\mathbf{d}}\langle G^K_Q\rangle_{\mathbf{d}}\exp(\mathrm{i}\mathbf{k}\cdot\mathbf{d}) \tag{6.6}$$

and,

$$\Psi^{K,u}_Q = \sum_{\mathbf{d}}\langle U^K_Q\rangle_{\mathbf{d}}\exp(\mathrm{i}\mathbf{k}\cdot\mathbf{d}), \tag{6.7}$$

where $\mathbf{k} = \mathbf{q} - \mathbf{q}'$ and the sum is over resonant ions. For Bragg diffraction, $\mathbf{k}$ coincides with a reciprocal lattice vector (h, k, l), and the sum is over resonant ions in a unit cell of the crystal.

Effecting the rearrangement of (6.5) into the sum of symmetric and antisymmetric components one arrives at,

$$Z(E1\text{–}M1) = AF(E1\text{–}M1),$$

Table 7. Components of $\tilde{M}^K_Q \pm M^K_Q$ with $\mathbf{q}' = \mathbf{q}$ that allow dichroic signals from $E1$–$M1$ events. The x-ray beam defines the z-axis which in spherical coordinates is the component 0.

$\tilde{M}^1_0 + M^1_0$	=	$-\mathrm{i}\sqrt{2}\hat{q}_0(\boldsymbol{\epsilon}' \cdot \boldsymbol{\epsilon})$
$\tilde{M}^2_{+2} + M^2_{+2}$	=	$2\mathrm{i}\hat{q}_0 X^2_{+2}$
$\tilde{M}^0_0 - M^0_0$	=	$-\mathrm{i}2\sqrt{2/3}\hat{q}_0 X^1_0$
	=	$\sqrt{2}\left(\tilde{M}^2_0 - M^2_0\right)$

Averaging over states of polarizations in the beam of x-rays leads to $(\boldsymbol{\epsilon}' \cdot \boldsymbol{\epsilon}) \to 1$, $\left(X^2_2\right)_{\mathrm{av}} = (P_3 + \mathrm{i}P_1)/2$ and $\left(X^1_0\right)_{\mathrm{av}} = -\hat{q}_0 P_2/\sqrt{(}2)$.

where A is a dimensionless constant, which contains reduced matrix elements of $\mathbf{R}$ and $\boldsymbol{\mu}$, and our structure factor is,

$$F(E1\text{–}M1) = \sum_{K=0,1,2} \mathrm{i}^{K-1} \sum_Q (-1)^Q \left\{ -\mathrm{i}\Psi^{K,g}_Q \left(\tilde{M}^K_{-Q} + M^K_{-Q} \right) + \Psi^{K,u}_Q \left(\tilde{M}^K_{-Q} - M^K_{-Q} \right) \right\}. \tag{6.8}$$

Equation (6.8) is our central result. It could be demanded simply by a previous analysis of $E1$–$E2$ events, with the range of K being one of two essential differences. The second essential difference between $E1$–$E2$ and $E1$–$M1$ structure factors is found in the x-ray factors, to which we turn our attention.

X-ray factors $\tilde{M}^K_Q$ and M^K_Q evaluated for our chosen geometry, in which the z-axis coincides with the x-ray wavevector $\mathbf{q}$ and the x-axis corresponds to $P_3 = +1$, are different from zero for projections $Q = 0, \pm 2$. One easily finds that polar tensors $K = Q = 0$ and $K = 2$, $Q = 0$ create natural circular dichroism. Using entries in table 7,

$$(\Delta F(E1\text{–}M1))_{\mathrm{av}} = \sqrt{\tfrac{2}{3}} P_2 \left\{ \sqrt{2}\Psi^{0,u}_0 - \Psi^{2,u}_0 \right\}. \tag{6.9}$$

The structure factors $\Psi^{K,u}_0$ for $\mathbf{k} = 0$ and with even K vanish if the point group includes a mirror as an element of symmetry. These structure factors are sums of pseudotensors $\langle U^0_0 \rangle$ and $\langle U^2_0 \rangle$, and the latter arises in $E1$–$E2$ dichroic signals discussed in the previous section. For a randomly oriented system, $\Psi^{2,u}_0 = 0$ while $\Psi^{0,u}_0$ is spherically symmetric and it can be different from zero for a randomly oriented system. For a single electron $U^0_0 \propto \mathbf{L} \cdot \boldsymbol{\Omega} = 0$. In consequence, non-zero natural circular dichroism in a randomly oriented system is a measure of two-electron correlations [15].

There are two possible contributions from magnetoelectric tensors to a dichroic signal, namely,

$$(\Delta F(E1\text{–}M1))_{\mathrm{av}} = -\sqrt{2}\hat{q}_0 \Psi^{1,g}_0 + \mathrm{i}\hat{q}_0 P_3 \left\{ \Psi^{2,g}_{-2} - \Psi^{2,g}_{+2} \right\}. \tag{6.10}$$

The magnetochiral and non-reciprocal linear dichroic $E1$–$M1$ signals shown in (6.10) have global symmetries already discussed in the context of $E1$–$E2$ signals. Here we mention behaviour of the dichroic signals (6.10) with respect to rotation of the sample relative to the beam. Rotation of the sample in a right-handed sense by an angle φ about the beam, defined by us to be the z-axis, simply multiplies Ψ^K_Q by a phase $\exp(-\mathrm{i}Q\varphi)$. Such a rotation evidently leaves the magnetochiral signal, $\Psi^{1,g}_0$, unchanged. However, the non-reciprocal linear dichroic signal, with $Q = -2$ and $+2$, acquires two phase factors $\exp(\pm 2\mathrm{i}\varphi)$. Rotations for which the phase factors are identical are $\varphi = \pi/2$ and the non-reciprocal linear dichroic signal changes sign, while for $\varphi = \pi$ the signal is unchanged. Other rotations of the sample of potential interest are π about the x-axis or y-axis. One can show that [9], for each of these rotations

the magnetochiral and non-reciprocal linear dichroic signals change sign. Hence, for the non-reciprocal signal (6.10), rotation of the sample by π about the x-axis or y-axis is equivalent to changing the direction of the beam, $\mathbf{q}_0 \rightarrow -\mathbf{q}_0$. Looking at the natural circular dichroic signal (6.9) one sees that it is unchanged by a rotation of the sample about the beam, because $Q = 0$, and, also, the signal is unchanged by rotation of the sample by π about the x-axis or y-axis. In contrast to the aforementioned behaviour of the natural circular dichroic signal, circular dichroic signals in (5.1) and (5.2) are unchanged by a rotation of the sample about the beam but change sign for rotation of the sample by π about the x-axis or y-axis, with the latter property a signature of a non-reciprocal signal.

In a report of measurements of absorption spectra of $GaFeO_3$ in the vicinity of the Fe K-edge, Kubota *et al* [62] refer to the sum of magnetochiral and non-reciprocal linear dichroic signals as directional dichroism. Spontaneous polarization and ferrimagnetism coexist in this orthorhombic piezoelectric material (space group $Pc2_1n$) when held below a magnetic transition temperature ≈200 K. An observed difference between absorption spectra recorded with opposite polarity of the spontaneous magnetization diminishes with increasing temperature of the sample, and it vanishes on passing through the transition temperature. This finding, and the measured change in the difference signal on rotation of the sample about the x-ray beam, is consistent with expressions in section 5 for magnetochiral and non-reciprocal linear dichroic signals created by an $E1$–$E2$ event. Similar experimental findings, deduced from the transmission spectrum in the optical range of energies (1.0–2.5 eV), are in complete accord with expression (6.10) for directional dichroism due to an $E1$–$M1$ event [63].

We conclude this discussion of $E1$–$M1$ events in dichroic signals and scattering by considering the extreme case of elastic backscattering for which $\mathbf{q} = -\mathbf{q}'$. Looking at the entries in table 7, x-ray tensors for backscattering are derived by changing the signs of M_Q^K. The four amplitudes that describe processes in the four polarization channels are now derived from all the resonant ions (scattering and not Bragg diffraction) and they are easily found to be,

$$F_{\substack{\sigma'\sigma \\ \pi'\pi}}(E1\text{–}M1) = \mp \mathrm{i}\sqrt{2}\Psi_0^{1,u} + \left\{\Psi_{-2}^{2,u} - \Psi_{+2}^{2,u}\right\} = \pm\alpha_3 + \beta, \tag{6.11}$$

$$F_{\substack{\pi'\sigma \\ \sigma'\pi}}(E1\text{–}M1) = \mp \mathrm{i}\left\{\Psi_{-2}^{2,u} + \Psi_{+2}^{2,u}\right\} + \frac{2}{\sqrt{3}}\left\{\Psi_0^{0,g} - \frac{1}{\sqrt{2}}\Psi_0^{2,g}\right\} = \pm\mathrm{i}\alpha_2 + \alpha_1. \tag{6.12}$$

Material information derived from dichroism, (6.9) and (6.10), is quite different from the information in elastic backscattering. Note that unrotated channels of scattering (6.11) contain only polar tensors. On the other hand, rotated channels (6.12) contain polar and magnetoelectric tensors, and the polar contribution, α_2, has opposite signs in the two channels $\pi'\sigma$ and $\sigma'\pi$. For a single electron, the magnetoelectric tensor $G_0^0 \propto \mathbf{L}\cdot\mathbf{n} = 0$ and scattering is therefore due to a two-electron contribution to (6.1). Tensor operators with $Q = 0$ are Hermitian and in (6.11) and (6.12) such operators are U_0^1, G_0^0 and G_0^2.

We have introduced in (6.11) and (6.12) variables α_1, α_2, α_3 and β that lead to neat expressions for the cross-section in terms of mean values of products of the variables, e.g. $\langle\beta^+\alpha_3\rangle$ and $\langle\beta^+\alpha_3\rangle^* = \langle\alpha_3^+\beta\rangle$ [2, 9]. Here, we give a result for the total scattered intensity, I, with linear (P_3) and circular (P_2) polarization in the primary beam. For $\mathbf{P} = (0, P_2, P_3)$, the total intensity in elastic backscattering by $E1$–$M1$ events is proportional to,

$$\begin{aligned} I = {} & \langle\boldsymbol{\alpha}^+\cdot\boldsymbol{\alpha}\rangle + \langle|\beta|^2\rangle + P_2\langle\beta^+\alpha_2 + \alpha_2^+\beta + \mathrm{i}(\alpha_3^+\alpha_1 - \alpha_1^+\alpha_3)\rangle \\ & + P_3\langle\beta^+\alpha_3 + \alpha_3^+\beta + \mathrm{i}(\alpha_1^+\alpha_2 - \alpha_2^+\alpha_1)\rangle. \end{aligned} \tag{6.13}$$

The magnetoelectric contribution to I, proportional to α_1, vanishes in the absence of magnetic order and it couples to an external magnetic field. Non-magnetic contributions proportional to

P_2 and P_3 have spatial signatures $xy(x^2 - y^2)$ and xyz, respectively (the z-axis is defined by the direction of the primary beam). The intensity (6.13) is associated with a Lorentzian energy profile.

7. Conclusion

In this paper we strive to highlight the close relationship between symmetry properties and their consequences for experimental observations in several layers of detail. Starting from the general assertion that the result for an experiment cannot, on the microscopic level, depend on the coordinates chosen for its description, we define two primary symmetries based on the isotropy of space and time, namely the behaviour under inversion and, independently, under time-reversal.

Most model experiments considered here employ circularly polarized (chiral or helical) x-rays as a probe for dichroism in solid and fluid matter, using absorption or resonant Bragg reflection events. Both kinds of experiment may be characterized by a scalar quantity, the scattering length f, which is necessarily invariant under symmetry transformations applied to the helical x-ray probe and the electronic properties of the sample.

The building blocks in our analysis of dichroism are, on the one hand, the behaviour of the photon wavevector and the helicity with respect to various symmetry transformations and, on the other hand, the behaviour of the electron variables under inversion and time-reversal. Thus, up to three variables may combine to give a dichroic signal and their required symmetry property is invariance under inversion and time-reversal. If these universal symmetries are augmented by additional symmetry transformations, we can deduct selection rules, or rather exclusion conditions, if these transformations affect only one part of the x-ray electron system (Neumann's principle). The results for forbidden and allowed dichroic signals are given in tables and the cases for ordered solids and fluids are discussed separately.

We find that, a surprising number of exclusion cases can be derived from symmetry properties, even before the details of the electronic system are taken into account. An atomic (model) calculation is required if we consider resonant Bragg reflection from crystalline solids, with a scalar unit cell structure factor F. In the forward direction F is proportional to a dichroic signal, we recall. Resonant Bragg reflection results from a two stage process in the electronic system and a detailed analysis shows that, the electron properties are represented by expectation values of equivalent tensor operators, in an approximation that is frequently valid in the analysis of observations. Scalar products of these multipoles with the corresponding x-ray variables constitute the essential parts of F. To display the effects of symmetry at this level of detail we consider a demonstrational model of a non-centrosymmetric cell. The final example is given by a new calculation of the structure factor for a (parity-odd) $E1$–$M1$ event. It is only when the atomic structure factor is recast into a new form, where the x-ray and electronic tensors exhibit their appropriate symmetry properties, that the various dichroic signals are recovered.

Acknowledgments

We have benefited from correspondence and discussion with Dr K S Knight and Professor G van der Laan.

Appendix A. Helicity operator and tensor products

The helicity operator $\Sigma = \mathrm{i}\mathbf{q} \cdot (\boldsymbol{\epsilon} \times \boldsymbol{\epsilon}^+)/q$, where $\mathbf{q}$ and $\boldsymbol{\epsilon}$ are the photon wavevector and polarization vector, respectively [16]. The time reversed polarization vector $= -\boldsymbol{\epsilon}^+$ where $^+$

denotes Hermitian conjugation and $\boldsymbol{\epsilon} \times \boldsymbol{\epsilon}^+$ is a square matrix. Also, Σ is a time-even operator by which we mean that it satisfies $(\theta \Sigma \theta^{-1})^+ = \Sigma$. An operator equivalent for Σ is the Pauli matrix σ_y.

An operator that changes sign under the combined action of the time-reversal and Hermitian conjugation operations is time-odd. Some authors choose not to include Hermitian conjugation in their definition of time-even and time-odd operators, in which case they are unable to give a unique time signature to non-Hermitian operators such as the spin raising operator $S_+ = -(S_x + \mathrm{i}S_y)/\sqrt{2}$.

If A^k_q and B^k_q are spherical tensors (or tensor operators) the tensor product $(A^k \otimes B^{k'})^K_Q$ defines a spherical tensor of rank K and projection Q. A standard definition of the tensor product is [59, 60],

$$(A^k \otimes B^{k'})^K_Q = \sum_{qq'} A^k_q B^{k'}_{q'} (kqk'q'|KQ), \tag{A.1}$$

where $(kqk'q'|KQ)$ is a Clebsch–Gordan coefficient. The coefficient is purely real, and it can be different from zero when $|k - k'| \leqslant K \leqslant k + k'$. The parity of the tensor product is the product of the parities of the two spherical tensors.

Let us explore properties of a tensor product of spherical harmonics $Y^k_q(\mathbf{R})$ and $Y^{k'}_{q'}(\mathbf{R}')$ [59, 61]. The action of inversion is $Y^k_q(-\mathbf{R}) = (-1)^k Y^k_q(\mathbf{R})$ and complex conjugation $\{Y^k_q(\mathbf{R})\}^* = (-1)^q Y^k_{-q}(\mathbf{R})$. It is convenient to introduce the notation,

$$\Phi^K_Q = (Y^k \otimes Y^{k'})^K_Q, \tag{A.2}$$

and the parity of Φ^K_Q is determined by $k + k'$. We assume that $\mathbf{R} \neq \mathbf{R}'$. For the particular case $\mathbf{R} = \mathbf{R}'$, Φ^K_Q vanishes unless $k + k' + K$ is even and these quantities are time-even, which follows by a specific application of a general rule that we shall now establish.

Action of the time-reversal operator on a classical quantity, like Φ^K_Q, is the same as complex conjugation. The Hermitian conjugate $\{\Phi^K_Q\}^+ = \{(\Phi^K_Q)^*\}^{\mathrm{T}}$, where the superscript $^{\mathrm{T}}$ denotes the transpose (elsewhere denoted by a tilde). As indicated above, the combination of complex and Hermitian conjugation $\{(\Phi^K_Q)^*\}^+ = \{(\Phi^K_Q)\}^{\mathrm{T}}$ provides our time signature for Φ^K_Q, and we have,

$$(\Phi^K_Q)^{\mathrm{T}} = (Y^{k'} \otimes Y^k)^K_Q = (-1)^{k+k'+K} \Phi^K_Q = \{(\Phi^K_Q)^*\}^+. \tag{A.3}$$

In (A.3) the second equality is a property of the Clebsch–Gordan coefficient. The third equality tells us that Φ^K_Q has a time signature determined by $k + k' + K$. In particular, if Φ^K_Q is parity-even there is a one to one correspondence between the rank and time signature. By way of an example, take $k = k' = K = 1$; one finds $\Phi^1_Q \propto \mathrm{i}(\mathbf{R} \times \mathbf{R}')_Q$ which is a spherical component of an axial vector, and it is time-odd because $k + k' + K$ is odd.

Turning to parity-odd Φ^K_Q, even K is time-odd and odd K is time-even. Thus, with $k + k'$ odd, for K even Φ^K_Q is equivalent to a magnetoelectric tensor, G^K_Q (K even), and with K odd Φ^K_Q is equivalent to a polar tensor, U^K_Q (K odd). For the remaining G^K_Q (K odd) and U^K_Q (K even) one may construct equivalents with a time-odd and parity-odd quantity, such as the anapole $\boldsymbol{\Omega}$. Alternatively, one can construct equivalents $(Y^{k''} \otimes \Phi^K_Q)^{K'}$, e.g., an equivalent for the pseudoscalar U^0 is derived from $k = k' = k'' = 1$, $K = 1$ and $K' = 0$ with $U^0 \propto \mathrm{i}(\mathbf{R} \times \mathbf{R}') \cdot \mathbf{R}''$. Hence a chiral measure of a material, U^0, involves three spatial coordinates and chirality is a non-local property.

Appendix B. Single-electron matrix elements

The building element in an atomic model of an $E1$–$M1$ resonant event is the product of matrix elements $\langle a|\boldsymbol{\epsilon}' \cdot \mathbf{R}|\eta\rangle\langle\eta|(\mathbf{q} \times \boldsymbol{\epsilon}) \cdot \boldsymbol{\mu}|a'\rangle$. We evaluate this product after representing the single-

electron states $|a\rangle$, $|a'\rangle$ and $|\eta\rangle$ by jm states, respectively, with total angular momentum j_1, j_2 and $\overline{J}$. The intermediate state $|\eta\rangle = |\overline{JM}\rangle$ is taken to be spatially isotropic with the product of matrix elements summed over the projections $\overline{M}$. One finds,

$$\begin{aligned}
&\sum_{\overline{M}} \langle a|\boldsymbol{\epsilon}' \cdot \mathbf{R}|\overline{JM}\rangle\langle\overline{JM}|(\mathbf{q}\times\boldsymbol{\epsilon})\cdot\boldsymbol{\mu}|a'\rangle \\
&\quad = \delta_{\bar{l},l_2} q \langle l_1|R|\bar{l}\rangle\langle\bar{l}|l_2\rangle (l_1\|C(1)\|l_2)(-1)^{1+\overline{J}-j_2}(2\overline{J}+1)[(2j_1+1)(2j_2+1)]^{1/2} \\
&\quad\times \left([l_2(l_2+1)(2l_2+1)]^{1/2} \begin{Bmatrix} l_2 & \overline{J} & 1/2 \\ j_2 & l_2 & 1 \end{Bmatrix} \right. \\
&\quad\left. + (-1)^{j_2-\overline{J}}\sqrt{6} \begin{Bmatrix} 1/2 & \overline{J} & l_2 \\ j_2 & 1/2 & 1 \end{Bmatrix} \right) \begin{Bmatrix} l_1 & j_1 & 1/2 \\ \overline{J} & l_2 & 1 \end{Bmatrix} \\
&\quad\times \sum_{KQ} (-1)^{K+Q}(2K+1)^{1/2} \begin{Bmatrix} j_1 & 1 & \overline{J} \\ 1 & j_2 & K \end{Bmatrix} \tilde{M}^K_{-Q} \\
&\quad\times (-1)^{j_1-m_1} \begin{pmatrix} j_1 & K & j_2 \\ -m_1 & Q & m_2 \end{pmatrix}. \qquad \text{(B.1)}
\end{aligned}$$

The x-ray spherical tensor $\tilde{M}^K_Q$ is defined in (6.2). Three main factors contribute to (B.1); the reduced matrix element of the dipole operator, $(j_1\|R\|\overline{J})$, the reduced matrix element of the magnetic moment operator, $(\overline{J}\|\mu\|j_2)$, and a recoupling of angular momentum states. The last factor is interpreted as a sum of matrix elements of a spherical tensor, Υ^K_Q, that satisfies Wigner–Eckart theorem with a reduced matrix element $(j_1\|\Upsilon(K)\|j_2)$ which is proportional to, $(-1)^K(2K+1)^{1/2}\begin{Bmatrix} j_1 & 1 & \overline{J} \\ 1 & j_2 & K \end{Bmatrix}$. The result (B.1) contains several selection rules. The intermediate state must have angular momentum l_2 and the radial overlap, $\langle\bar{l}|l_2\rangle$, must be different from zero. Both these conditions arise from the matrix element of the magnetic moment. Note that the latter is not zero at the K-edge, for which $\bar{l} = l_2 = 0$ and $(j_2\|\mu\|j_2) = g(j_2\|j\|j_2)$ with the Landé factor $g = 2$ and $(j_2\|j\|j_2) = \sqrt{3/2}$. The reduced matrix elements of a spherical harmonic $(l_1\|C(t)\|l_2)$ vanish unless l_1+t+l_2 is an even integer. Thus, the dipole matrix element in (B.1) vanishes unless $l_1 + l_2 = 2n + 1$, which states that allowed events are parity-odd ($t = 1$).

References

[1] Fasman G D (ed) 1996 *Circular Dichroism and Conformal Analysis of Biomolecules* (New York: Plenum)
[2] Lovesey S W and Collins S P 1996 *X-ray Scattering and Absorption by Magnetic Materials* (Oxford: Clarendon)
[3] Rodger A and Norden B 1997 *Circular Dichroism and Linear Dichroism* (Oxford: Oxford University Press)
[4] Berova N, Nakanishi K and Woody R W (ed) 2000 *Circular Dichroism. Principles and Applications* (New York: Wiley–VCH)
[5] Barron L D 2004 *Molecular Light Scattering and Optical Activity* (Cambridge: Cambridge University Press)
[6] van der Laan G 2006 *Lect. Notes Phys.* **697** 143
[7] Srajer G *et al* 2006 *J. Magn. Magn. Mater.* **307** 1
[8] Als-Nielsen J and McMorrow D 2001 *Elements of Modern X-ray Physics* (New York: Wiley)
[9] Lovesey S W, Balcar E, Knight K S and Fernández Rodríguez J 2005 *Phys. Rep.* **411** 233
[10] Dubovik V M and Tugushev V V 1990 *Phys. Rep.* **187** 145
[11] Birss R R 1964 *Symmetry and Magnetism* (Amsterdam: North-Holland)
Cracknell A P 1975 *Magnetism in Crystalline Materials* (Oxford: Pergamon)
[12] Nye J F 1985 *Physical Properties of Crystals* (Oxford: Clarendon)
[13] Burns G and Glazer A M 1990 *Space Groups for Solid State Scientists* (Boston, MA: Academic)
[14] Sakurai J J 1987 *Advanced Quantum Mechanics* (Redwood: Addison-Wesley)
[15] Carra P and Benoist R 2000 *Phys. Rev.* B **62** R7703
Marri I, Carra P and Bertoni C M 2006 *J. Phys. A: Math. Gen.* **39** 1969

[16] Landau L D and Lifshitz E M 1982 *Quantum Electrodynamics* 2nd edn vol 4, (Oxford: Pergamon)
[17] Brouder Ch 1990 *J. Phys.: Condens. Matter* **2** 701 and references therein
[18] van Vleck J H 1966 *The Theory of Electric and Magnetic Susceptibilities* (Oxford: Oxford University Press)
[19] Mason S F 1982 *Molecular Optical Activity and the Chiral Discriminations* (Cambridge: Cambridge University Press)
[20] Eliel E L and Wilen S H 1994 *Stereochemistry of Organic Compounds* (New York: Wiley)
[21] Lough W J and Wainer I W 2002 *Chirality in Natural and Applied Science* (Oxford: Blackwell Science)
[22] Thomson W 1904 *Baltimore Lectures* (London: C J Clay & Sons) reprinted from 1893 *The Robert Boyle Lecture* Oxford University Junior Scientific Club
[23] Pasteur L 1848 *Ann. Chim. Phys.* **24** 442
[24] Abrahams S C, Glass A M and Nassua K 1977 *Solid State Commun.* **24** 515
[25] Brown P J and Forsyth J B 1996 *Acta Crystallogr.* A **52** 408
[26] Viedma C 2005 *Phys. Rev. Lett.* **94** 065504
[27] Lovesey S W 1987 *Theory of Neutron Scattering from Condensed Matter* vol 2 (Oxford: Clarendon)
[28] Sears V F 1986 *Phys. Rep.* **141** 281
[29] Bonner W A 1991 The origin and amplification of biomolecular chirality *Origin of Life and Evolution of the Biosphere* **21** 59
[30] Day C 2005 *Phys. Today* **58** 21
[31] Rikken G L J A and Raupach E 2000 *Nature* **405** 932
[32] von Neumann F E 1885 *Vorlesungen über die Theorie Elastizität der festen Körper und des Lichtäthers* (Leipzig: Teubner)
[33] Abragam A and Bleaney B 1970 *Electron Paramagnetic Resonance of Transition Ions* (Oxford: Clarendon Press)
[34] Tranter G E 1985 *Nature* **318** 172
[35] Khriplovich I B 1991 *Parity Nonconservation in Atomic Phenomena* (Philadelphia, PA: Gordon and Breach)
[36] Natoli C R *et al* 1998 *Eur. J. Phys.* B **4** 1
[37] Alagna L *et al* 1998 *Phys. Rev. Lett.* **80** 4799
[38] Goulon J *et al* 1998 *J. Chem. Phys.* **108** 6394
[39] Carra P, Jerez A and Marri I 2003 *Phys. Rev.* B **67** 045111
[40] Di Matteo S, Joly Y and Natoli C R 2005 *Phys. Rev.* B **72** 144406
[41] Goulon J *et al* 2002 *Phys. Rev. Lett.* **88** 237401
[42] Di Matteo S and Natoli C R 2002 *Phys. Rev.* B **66** 212413
[43] Di Matteo S, Joly Y and Natoli C R 2003 *Phys. Rev.* B **67** 195105
[44] Goulon J *et al* 2000 *Phys. Rev. Lett.* **85** 4385
[45] Yoshida K 1996 *Theory of Magnetism* (Berlin: Springer)
[46] Dmitrienko V E 1983 *Acta Crystallogr.* A **39** 29
Dmitrienko V E 1984 *Acta Crystallogr.* **40** 89
[47] Templeton D H and Templeton L K 1985 *Acta Crystallogr.* A **41** 133
Templeton D H and Templeton L K 1985 *Acta Crystallogr.* **41** 365
Templeton D H and Templeton L K 1986 *Acta Crystallogr.* **42** 478
[48] Ovchinnikova E N and Dmitrienko V E 2000 *Acta Crystallogr.* **56** 2
[49] Thole B T *et al* 1992 *Phys. Rev. Lett.* **68** 1943
[50] Carra P *et al* 1993 *Phys. Rev. Lett.* **70** 694
[51] Lovesey S W and Balcar E 1996 *J. Phys.: Condens. Matter* **8** 10983
[52] Lovesey S W 1996 *J. Phys.: Condens. Matter* **8** 11009
[53] Lovesey S W 1998 *J. Phys.: Condens. Matter* **10** 2505
[54] Lovesey S W and Balcar E 1997 *J. Phys.: Condens. Matter* **9** 4237
[55] Brown P J *et al* 2002 *J. Phys.: Condens. Matter* **14** 1957
[56] Muto M *et al* 1998 *Phys. Rev.* B **57** 9586
[57] Di Matteo S *et al* 2003 *Phys. Rev. Lett.* **91** 257402
[58] Turchini S, Zema N, Zennaro S, Alagna L, Stewart B, Peacock R D and Prosperi T 2004 *J. Am. Chem. Soc.* **126** 4532
[59] Edmonds A R 1960 *Angular Momentum in Quantum Mechanics* (Princeton, NJ: Princeton University Press)
[60] Judd B R 1963 *Operator Techniques in Atomic Spectroscopy* (New York: McGraw-Hill)
[61] Varshalovich D A, Moskalev A N and Khersonskii V K 1988 *Quantum Theory of Angular Momentum* (Singapore: World Scientific)
[62] Kubota M *et al* 2004 *Phys. Rev. Lett.* **92** 137401
[63] Jung J H *et al* 2004 *Phys. Rev. Lett.* **93** 037403